

Fast Visible-Light 3D Printing of Conductive PEDOT:PSS Hydrogels

Naroa Lopez-Larrea, Antonela Gallastegui, Luis Lezama, Miryam Criado-Gonzalez, Nerea Casado, and David Mecerreyes*

Functional inks for light-based 3D printing are actively being searched for being able to exploit all the potentialities of additive manufacturing. Herein, a fast visible-light photopolymerization process is showed of conductive PEDOT:PSS hydrogels. For this purpose, a new Type II photoinitiator system (PIS) based on riboflavin (Rf), triethanolamine (TEA), and poly(3,4-ethylenedioxythiophene):poly(styrenesulfonate) (PEDOT:PSS) is investigated for the visible light photopolymerization of acrylic monomers. PEDOT:PSS has a dual role by accelerating the photoinitiation process and providing conductivity to the obtained hydrogels. Using this PIS, full monomer conversion is achieved in less than 2 min using visible light. First, the PIS mechanism is studied, proposing that electron transfer between the triplet excited state of the dye ($^3Rf^*$) and the amine (TEA) is catalyzed by PEDOT:PSS. Second, a series of poly(2-hydroxyethyl acrylate)/PEDOT:PSS hydrogels with different compositions are obtained by photopolymerization. The presence of PEDOT:PSS negatively influences the swelling properties of hydrogels, but significantly increases its mechanical modulus and electrical properties. The new PIS is also tested for 3D printing in a commercially available Digital Light Processing (DLP) 3D printer (405 nm wavelength), obtaining high resolution and 500 μm hole size conductive scaffolds.

1. Introduction

In the last few years, conductive hydrogels have emerged as promising materials for the next generation bioelectronic interfaces; artificial skin, flexible and implantable bioelectronics, and tissue engineering. This interest is due to their similarities to biological tissues and electrical, mechanical, and biofunctional properties.^[1–11] However, it is still a challenge to formulate hydrogels with high electrical conductivity without compromising their physicochemical properties (e.g., stretchability and toughness).^[12,13] The most commonly used conductive polymers (CPs) for the synthesis of conductive hydrogels are polyaniline (PANI), polypyrrole (PPy) and poly(3,4-ethylenedioxythiophene) doped with poly(styrenesulfonate) (PEDOT:PSS), although certain carbon nanomaterials such as carbon nanotubes (CNTs) and graphene are also widely used for the synthesis of conductive hydrogels.


Among them, the most popular conducting polymer for these applications is PEDOT:PSS due to its high conductivity,

stability, and biocompatibility.^[14] However, PEDOT:PSS is insoluble and infusible, thus, the synthesis of 3D conductive materials is still a challenge.^[15,16] For that reason, additive manufacturing 3D printing methods are increasingly being used in order to create conductive hydrogels using different type of techniques such as inkjet printing,^[17,18] extrusion-based printing^[19–21] and light-based printing.^[22–24] Very recently, we have shown that PEDOT can be copolymerized with poly(ϵ -caprolactone) (PCL) biopolymer, leading to PEDOT-g-PCL graft copolymers. This copolymer shows excellent shear-thinning behavior to be processed by extrusion-based printing in order to synthesize 3D scaffolds to induce muscle cells (myotubes) differentiation.^[25] In another example, we have dispersed PEDOT:PSS in an aqueous matrix formed by vinyl resins in order to photopolymerize flexible and shape-defined conductive hydrogels for application as bioelectrodes for human electrocardiography (ECG) and electromyography (EMG) recordings, showing long-term activity and enhanced detection signals compared to commercial Ag/AgCl medical electrodes for health monitoring.^[26] However, these strategies to obtain 3D conductive hydrogels are still far from being easy and rapid methodologies.

N. Lopez-Larrea, A. Gallastegui, M. Criado-Gonzalez, N. Casado, D. Mecerreyes
 POLYMAT
 University of the Basque Country UPV/EHU
 Avenida Tolosa 72, Donostia-San Sebastian, Guipuzcoa 20018, Spain
 E-mail: david.mecerreyes@ehu.es

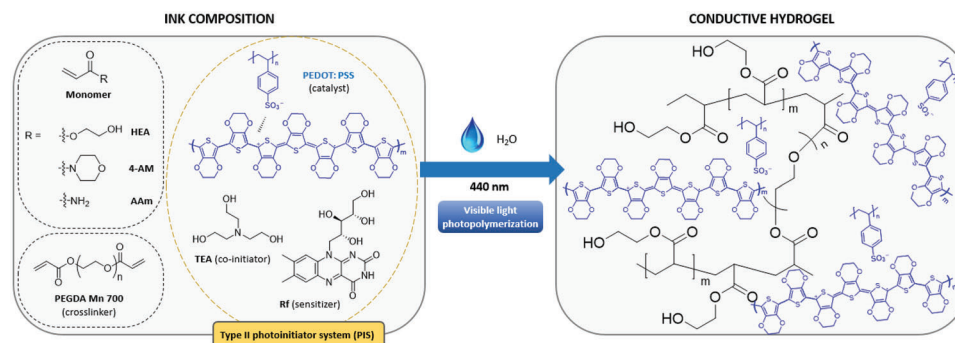
L. Lezama
 Departamento de Química Orgánica e Inorgánica
 University of the Basque Country UPV/EHU
 Barrio Sarriena s/n, Leioa, Bizkaia 48940, Spain

N. Casado, D. Mecerreyes
 IKERBASQUE
 Basque Foundation for Science
 Plaza Euskadi 5, Bilbao 48009, Spain

 The ORCID identification number(s) for the author(s) of this article can be found under <https://doi.org/10.1002/marc.202300229>

© 2023 The Authors. Macromolecular Rapid Communications published by Wiley-VCH GmbH. This is an open access article under the terms of the Creative Commons Attribution License, which permits use, distribution and reproduction in any medium, provided the original work is properly cited.

DOI: 10.1002/marc.202300229



Scheme 1. Schematic representation of the main reagents involved in the visible light photopolymerization reaction.

Light-based 3D printing encompasses the additive manufacturing methods with the highest resolution (between 20 and 100 μm).^[27] Here, photoinitiators that absorb in the UV range are usually employed to formulate different conductive inks. However, the use of UV light in photopolymerization processes has some drawbacks; for example, it can damage user's health and can produce ozone when the oxygen of the atmosphere is irradiated with UV light.^[28] For that reason, photoinitiating systems that can be activated under low light intensity and in the visible range (400–700 nm) have been researched in the recent years.^[29–33] The use of visible light sources such as Light-Emitting Diodes (LEDs) in photopolymerization processes instead of UV light provides a number of advantages such as low energy consumption, room temperature treatment, non-polluting, low-costs, and solvent-free formulations.^[28] Additionally, light penetration is limited to $\approx 600 \mu\text{m}$ in the UV range, while using higher wavelengths it increases up to 2 cm, evidencing the interest of polymerizing under visible light.^[34] However, visible light photoinitiators are usually not fast enough to be used in light-based 3D printing methods. This happens because UV light and visible light photoinitiators have a different mechanism to produce active radicals.^[35] The photopolymerization reactions using visible light are usually promoted by Type II photoinitiator systems (PISs), where a sensitizer absorbs photons from the visible light source and then it transfers the energy to a co-initiator (hydrogen donor) by a hydrogen abstraction reaction. During this reaction, active radical species and sensitizer radicals are generated, but only the active radical species initiate the free radical polymerization.^[36–38] Thus, the initiating efficiency of Type II PISs is slower than the one of Type I photoinitiators, which are based on unimolecular formation of radicals. Furthermore, Type II PISs often require the absence of oxygen (a radical polymerization inhibitor), the absence of absorbent additives that could also absorb visible light, and high exposure times.^[39] Therefore, the development of a fast visible light photoinitiator system (PIS) for light-based 3D printing methods is needed in order to synthesize conductive hydrogels in a fast and secure way.

The goal of this article is to propose a new fast visible-light PIS in the presence of PEDOT:PSS, which allows the preparation of 3D conducting hydrogels by light-based 3D printing extending the range of conducting polymer materials and inks for additive manufacturing. The visible-light PIS is composed of Riboflavin (Rf) as the sensitizer, commonly known as the water-soluble vitamin B₂,^[40] triethanolamine (TEA) as the co-

initiator, and PEDOT:PSS conductive polymer as catalyst, as illustrated in **Scheme 1**. This new Type II PIS PEDOT:PSS/Rf/TEA was employed in the polymerization of various monomers such as 2-hydroxyethyl acrylate (HEA), 4-acryloyl morpholine (4-AM) and acrylamide (AAm), using a little amount of polyethylene glycol diacrylate (PEGDA Mn 700) as a cross-linker agent. Using a visible light irradiation source of 440 nm and power of 2 mW cm^{-2} , poly(hydroxyethyl acrylate) (PHEA) hydrogels containing PEDOT:PSS were obtained in less than 1 min.

2. Results and Discussion

In our previous work, CNTs were employed in the PIS system.^[39] Surprisingly, the use of PEDOT:PSS instead of CNTs in the Type II PIS makes the photopolymerization reaction faster. For that reason, photopolymerization reaction kinetics of different pre-polymeric mixtures were investigated (Table S1, Supporting Information). On the one hand, these pre-polymeric mixtures, which need in situ preparation, were composed of Monomer/PEGDA in a ratio of 90/10 (50 wt.% of the total ink formulation), and an aqueous solution of different conductive species at 1.3 wt.% (the remaining 50 wt.% of the ink). As for the concentration of Rf and TEA, the co-initiator TEA was used at a concentration of 0.2 M and Rf was used at a concentration of 1E-05 M according to Encinas et al., who investigated the polymerization rates of 2-hydroxyethyl methacrylate (HEMA) photoinitiated by riboflavin using as co-initiator several concentration of different amines (triethanolamine, triethylamine, dibutylamine, and dimethylamine).^[41] They obtained faster kinetics using TEA as the co-initiator and they conclude that the photochemical efficiency is strongly dependent on the structural features of the amines, therefore, triethanolamine was chosen as the standard co-initiator. On the other hand, the kinetics were followed by Fourier Transform Infrared Spectroscopy (FTIR), irradiating with visible light (440 nm, 2 mW cm^{-2}) the different inks and following the disappearance of C=C out of plane bending vibration (vinyl peak) of the monomer at 990 cm^{-1} (Figure S1A, Supporting Information). LEDs of 440 nm were used as irradiation source as it is the maximum absorption wavelength of riboflavin, the molecule that acts as sensitizer in the system.^[40]

First of all, various inks containing different conducting species (PEDOT:PSS, CNTs, polyaniline PANi and poly(3-hexylthiophene-2,5-diyl) P3HT) were analyzed. Results reveal that when PEDOT:PSS is used, full conversion is reached in

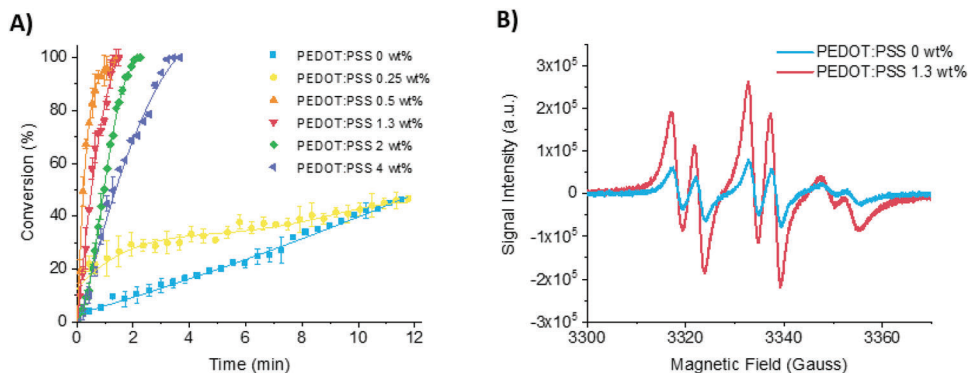


Figure 1. A) Evolution of the photopolymerization reaction kinetics given by % 2-Hydroxyethyl acrylate HEA monomer conversion versus irradiation time (min) of various pre-polymeric mixtures using different PEDOT:PSS concentration. B) EPR spectra for PEDOT:PSS 0 and 1.3 wt.% inks (containing PBN spin trap) after 60 s of irradiation.

1 min. However, when other conducting materials are employed, the irradiation time to get 100% conversion extends to 10–12 min (Figure S1B, Supporting Information). This behavior can be explained by the conductivity values of the different CP dispersions that are used. Table S2 (Supporting Information) shows the electrical conductivity of drop-casted CP dispersions. While PEDOT:PSS has a conductivity value of 100 mS cm^{-1} , the other conductive species (CNTs, PANi and P3HT) have conductivities of 3 orders of magnitude lower. Therefore, the electrical conductivity of the CP that is used seems important for the rapid photopolymerization kinetics being PEDOT:PSS the one that shows better results.

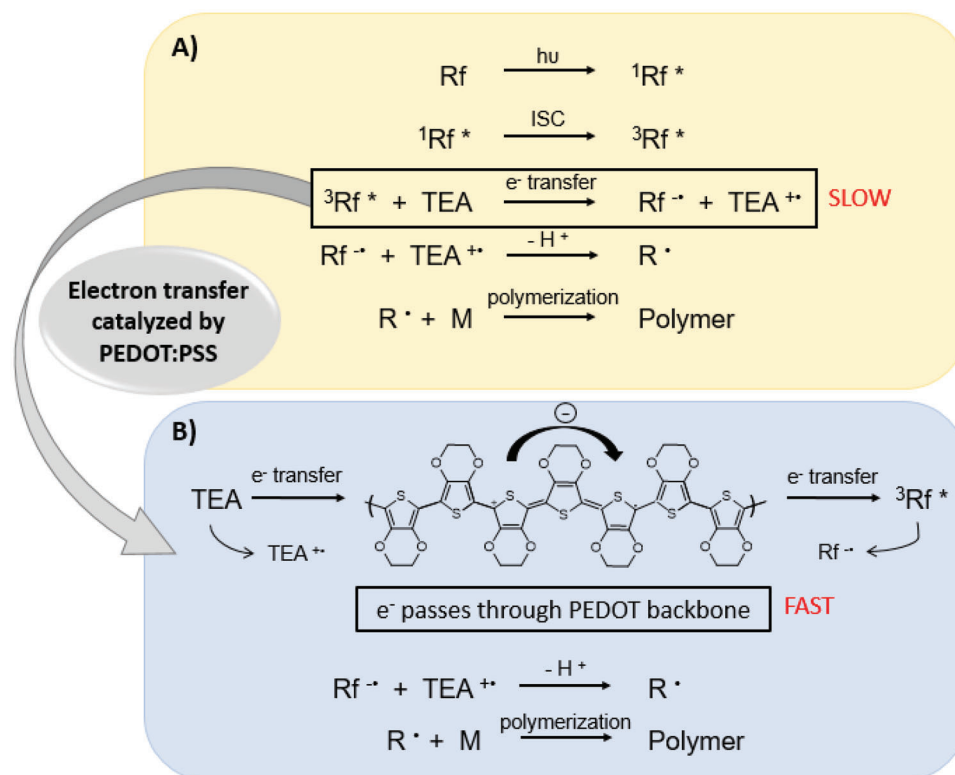
In a next step, photopolymerization reaction kinetics were analyzed using different monomers (HEA, 4-AM, PEGDA, and AAm) and PEDOT:PSS. In this case, all inks reached full conversion in 1 min, except for 4-AM pre-polymeric mixture that took twice as long (2 min) to get 100% conversion (Figure S1C, Supporting Information). This can be explained by the fact that 4-AM is more hydrophobic than HEA, PEGDA, and AAm monomers. Therefore, it interacts in a less effective way with the new water-soluble Type II PIS, and hence, kinetics of photopolymerization reaction are slower. Besides, poly(2-hydroxyethyl acrylate) (PHEA) has a lower glass transition temperature (T_g) than the other studied polymers, so the obtained hydrogels could meet the requirement of soft mechanical properties for bioelectronic application.^[42] For that reason, HEA was chosen as the standard monomer for next experiments.

To better understand the role of PEDOT:PSS in the system, additional kinetic studies were carried out using as the PIS only Rf/TEA, Rf/PEDOT:PSS and TEA/PEDOT:PSS (Figure S1D, Supporting Information). In the case of Rf/PEDOT:PSS and TEA/PEDOT:PSS, the polymerization did not occur. However, using the conventional Type II PIS, Rf/TEA without PEDOT:PSS, the kinetics were very slow, obtaining only a 40% of conversion in 12 min. Therefore, PEDOT:PSS only increases up the photopolymerization speed when all of the PIS components are present in the system and does not initiate the photopolymerization reaction. In order to confirm that riboflavin, which maximum absorbance wavelength is 445 nm,^[40] is the molecule that initiate the photopolymerization and that PEDOT:PSS, which absorbs in all the visible range,^[43] only speeds up the photopoly-

merization reaction, some kinetic measurements of PEDOT:PSS 1.3 wt.% ink were performed using 525 and 660 nm wavelengths (Figure S1E, Supporting Information). As expected, using green and red-light sources, photopolymerization does not occur, confirming again Type II general photoinitiator mechanism.

Finally, the effect of the PEDOT:PSS concentration on the photopolymerization reaction kinetics was studied. Figure 1A shows the kinetics of some pre-polymeric mixtures employing 0, 0.25, 0.5, 1.3, 2, and 4 wt.% PEDOT:PSS. Results reveal that at least 0.5 wt.% PEDOT:PSS is necessary to accelerate the photopolymerization reaction. However, when the concentration of PEDOT:PSS increases up to 4 wt.%, the time to reach a full conversion is extended from 1 to 4 min. This behavior may occur as a result of a deep curing effect. PEDOT:PSS absorbs in the visible range, therefore, as the concentration of PEDOT:PSS increases in the system, Rf and PEDOT:PSS compete for the absorbance of photons and the speed of the photopolymerization slows down. Figure S2 (Supporting Information) shows the normalized absorbance of different pre-polymeric mixtures containing different concentrations of PEDOT:PSS in the visible range.

Many factors could be contributing to the important increase in the polymerization rate using the PEDOT:PSS/Rf/TEA PIS. On the one hand, as known for Rf/TEA Type II photoinitiator system, there is an electron transfer between the triplet excited state of the dye ($^3\text{Rf}^*$) and the amine (TEA) followed by a fast proton abstraction.^[39] In this way, active amino radicals (R^*) are formed and chain reaction starts (Scheme 2A). On the other hand, we hypothesize that PEDOT:PSS conducting polymer, whose structure is already oxidized, could catalyze this electron transfer between $^3\text{Rf}^*$ and TEA (Scheme 2B), thus increasing the reaction speed.^[14,44] It is worth noting that PEDOT:PSS only acts as electron conductor in the mechanism, and it remains with the same redox structure after photopolymerization, giving blue color to the final hydrogel.^[45] Another consideration to bear in mind is that PEDOT:PSS must be also well dispersed in the aqueous pre-polymeric mixture in order to be in close contact with Rf and TEA. It is well known that PEDOT:PSS swells in aqueous media, and as Rf and TEA are solubilized in the aqueous solution, the interaction between the PEDOT:PSS surface and all PIS components is high enough to speed up the photopolymerization reaction.^[46–48]



Scheme 2. Visible light photoinitiator mechanism for vinyl polymerization employing A) the known Type II photoinitiator system Rf/TEA and B) the proposed paths when PEDOT:PSS intervene in the process.

This closeness would avoid diffusional steps and the possible inhibition of oxygen in the system.

To clarify the role of PEDOT:PSS in the photopolymerization mechanism, electron paramagnetic resonance (EPR) experiments were carried out. First of all, the EPR spectrum of PEDOT:PSS 0.5 wt.% aqueous solution was recorded, as PEDOT:PSS itself gives a single isotropic signal at $g = 2.0030$ (see Figure S3A, Supporting Information). Then, the spectra of two pre-polymeric solutions (PEDOT:PSS 0 wt.% and PEDOT:PSS 1.3 wt.%) containing *N*-tert-butyl- α -phenylnitron (PBN) spin trap were recorded at different irradiation times at room temperature. These two samples were compared at 60 s of irradiation time, and it can be seen that the EPR signal of PEDOT:PSS containing sample is more intense (see Figure 1B). The observed spectra could be well fitted with $g = 2.0058$ and $A_N = 16.5$ G (see Figure S3B, Supporting Information), in good agreement with what is expected for a nitron radical, the intensity of the lines being quantitatively related to the number of radicals that the photopolymerization system is creating. Therefore, it is demonstrated that the presence of PEDOT:PSS in the Type II PIS accelerates the radical generation reaction. Moreover, the creation of radicals in the PEDOT:PSS containing sample was also followed by EPR. Figure S4 (Supporting Information) shows the EPR spectra of the sample at different irradiation times (0, 30, and 60 s), and it can be seen that the intensity of the signal increases with time. These experiments confirm the proposed mechanism in Scheme 2, where PEDOT:PSS catalysis the electron transfer be-

tween ${}^3\text{Rf}^*$ and TEA, favoring the creation of active radicals to initiate the polymerization.

Therefore, as the presence of PEDOT:PSS clearly influences the kinetics of the system, PHEA hydrogels were synthesized with 0, 0.5, 1.3, and 2 wt.% PEDOT:PSS (the most rapid formulations, see Figure S5, Supporting Information) in order to determine how the electrochemical and mechanical properties of hydrogels change with PEDOT:PSS concentration. It is very important to study these properties as the conductive hydrogels are potential materials for application in bioelectronics, where good electrical conductivity is needed for biosensing and soft mechanical properties are needed to mimic human tissue.

Figure 2A presents the swelling behavior in water versus time, an important feature of hydrogels that describes their ability to retain water. It can be noted that the maximum water uptake capacity of the hydrogels is achieved in 2 h. Moreover, as PEDOT:PSS concentration increases in the polymeric matrix, the swelling ratio decreases continuously, from $362 \pm 10\%$ for PEDOT:PSS 0 wt.% hydrogel to $236 \pm 12\%$ for PEDOT:PSS 2 wt.%. These results are expected due to the addition of PEDOT:PSS hydrophobic additive in the PHEA hydrogel structure. Overall, different swelling values can be achieved changing the concentration of PEDOT:PSS, which can be advantageous for different applications such as sensing or cell culture.^[49–51]

Interestingly, the electrical conductivity of PHEA/PEDOT:PSS hydrogels was measured by the 4-Point Probe method, and results are shown in Figure 2B. Obviously, as the PEDOT:PSS

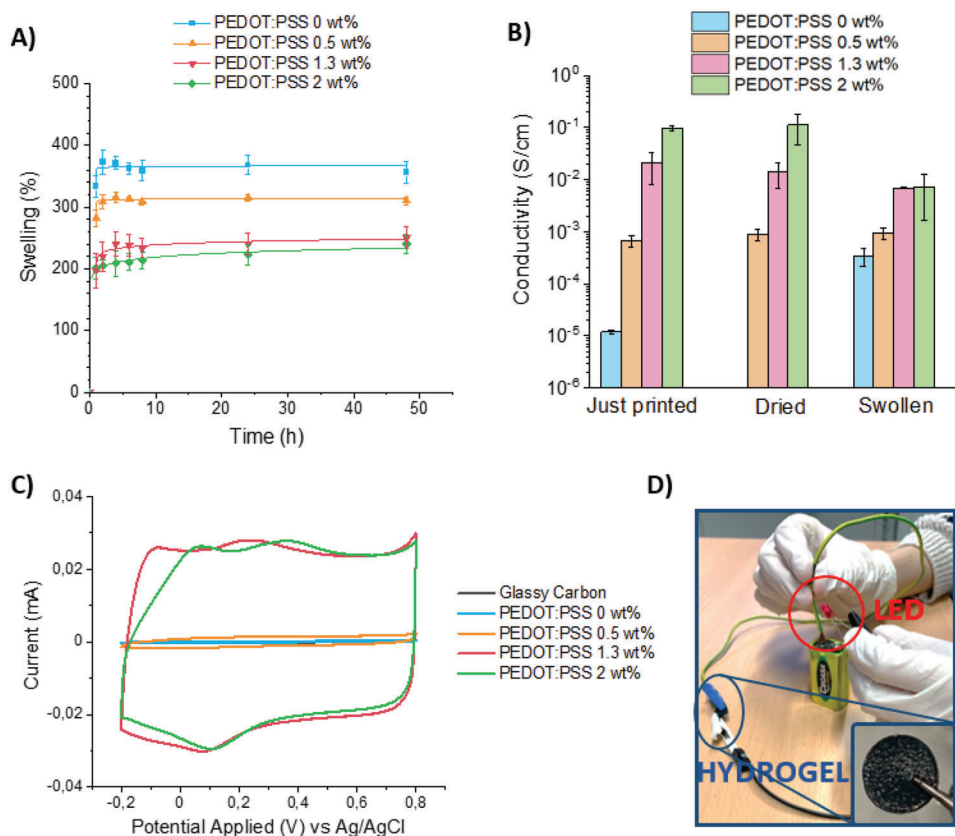


Figure 2. A) Swelling curves in water, B) Electrical conductivity in dried/swollen state and C) Cyclic voltammograms over a glassy carbon electrode in 0.1 M NaCl aqueous solution at 20 mV s⁻¹ of PHEA hydrogels containing 0, 0.5, 1.3, and 2 wt.% PEDOT:PSS. D) Lab-made electrical circuit to conduct the electrical current from the battery to the LED (red), passing through the PHEA hydrogel containing 1.3 wt.% PEDOT:PSS (blue).

concentration increases, so does the conductivity, as observed in other related works,^[22,52–54] reaching 0.1 S cm⁻¹ for the hydrogel containing 2 wt.% PEDOT:PSS, similar value as the commercial PEDOT:PSS (Heraeus PH1000). Conductivity of hydrogels was also measured in their swollen state. In this case, the conductivity value decreases almost one order of magnitude for all samples comparing with their dried state. It is worth noting that the hydrogel without PEDOT:PSS used as control only shows low conductivity values in its swollen state due to the ionic conductivity and it does not show electrical conductivity in its dry state, as expected, proving the key role of PEDOT:PSS in the hydrogels for conductive purposes.

The electroactive behavior of hydrogels was also tested by cyclic voltammetry in 0.1 M NaCl aqueous solution (Figure 2C; Figure S6, Supporting Information). Only the cyclic voltammograms (CV) of the hydrogels containing 1.3 and 2 wt.% PEDOT:PSS show a capacitive behavior, with a broad anodic peak between 0.2 and 0.4 V and a broad cathodic peak at 0.1 V, not observed in the case of hydrogels containing 0 and 0.5 wt.% PEDOT:PSS (Figure 2C). These results can be compared with the electrical conductivity measurements when hydrogels are swollen, whose tendency is the same. Moreover, the CVs of PEDOT:PSS 1.3 wt.% hydrogel at different scan rates show a proportional increase of the anodic and cathodic currents with the scan rate, which means that the redox processes are not limited by dif-

fusion and the whole hydrogel is involved in the electro-chemical processes (Figure S6, Supporting Information).

As a visual proof-of-concept of hydrogel's electrical properties, a lab-made electrical circuit that incorporates the synthesized hydrogel was built (see Figure 2D). The hydrogel is able to transfer the electrical current from the battery to the LED switching it on.

The presence of PEDOT:PSS also affected the mechanical properties of the PHEA hydrogels, as observed in Figure 3A and Figure S7 (Supporting Information). It can be seen that storage modulus (G') and loss modulus (G'') do not intersect between them, which means that the hydrogels behave like a solid in all the frequency range. Moreover, the storage modulus (G') increases from 9.3E + 04 Pa to 8.1E + 05 Pa (at 1 Hz frequency and 25 °C), obtaining a harder material as the concentration of PEDOT:PSS increases in the polymer matrix. Figure 3B shows the stress-strain curves of the synthesized materials with Type V probe shape (Figure 3C) obtained from the tensile test experiment. As the PEDOT:PSS quantity increases in the system, the Young's Modulus also increases from 0.24 ± 0.03 to 1.52 ± 0.40 MPa, for PEDOT:PSS 0 and 2 wt.% matrixes, respectively (Figure S8, Supporting Information). In the same way, the elongation at break decreases from 34 ± 2 to 23 ± 5% with the addition of PEDOT:PSS in the matrix. Even though the incorporation of PEDOT:PSS makes the hydrogels to be harder, the

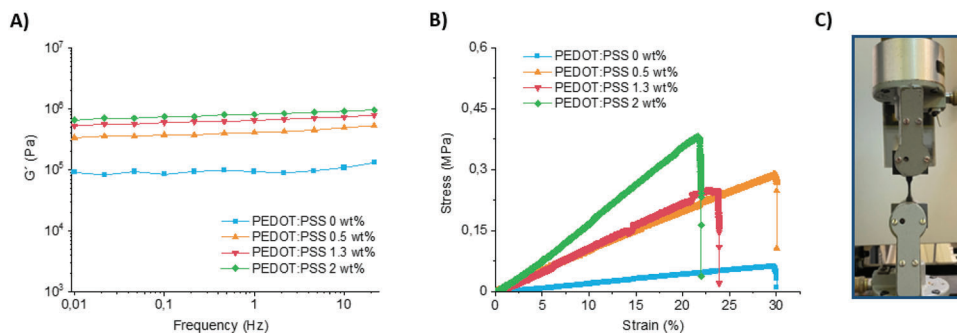


Figure 3. A) Matrix characterization by dynamic mechanical analysis (DMA) and B) Stress–strain curves of synthesized materials containing 0, 0.5, 1.3, and 2 wt.% PEDOT:PSS. C) Representative picture of the 1.3 wt.% PEDOT:PSS hydrogel with a Type V probe shape before the tensile test analysis.

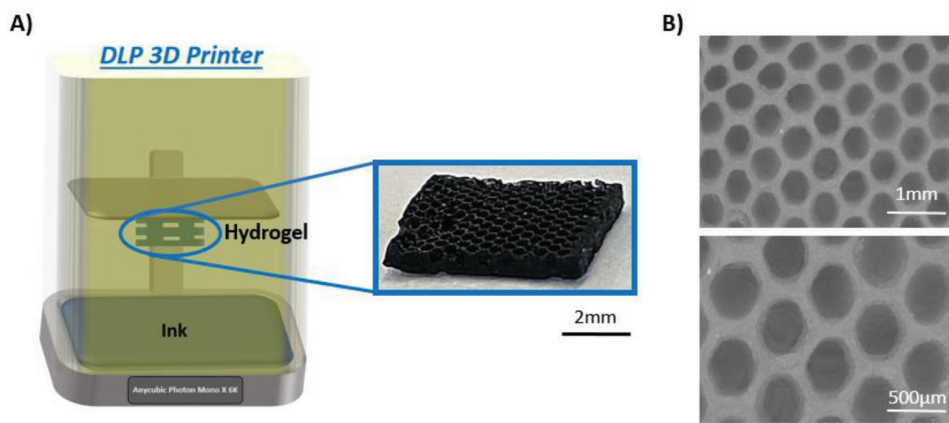


Figure 4. A) Representative scheme of the 3D printer system and a picture of the 3D printed honeycomb hydrogel. B) SEM images of the printed honeycomb hydrogel.

materials are still flexible for some biological applications such as biosensing.^[55]

Finally, the new PIS based on PEDOT:PSS/Rf/TEA was tested for 3D printing to prove that the new Type II PIS is comparable to other reported methods,^[56,57] employing the PEDOT:PSS 1.3 wt.% pre-polymeric mixture (using HEA as monomer) and a commercially available DLP (Digital Light Processing) 3D printer, Any Cubic Photon Mono X 6K model (wavelength = 405 nm and power = 2 mW cm⁻²). Although riboflavin can absorb also at 405 nm, the most efficient printabilities are obtained with blue light, for which new visible light 3D printers are being developed in order to maximize the efficiency of Type II PIS like the one explored here, to photopolymerize in a secure way and not damaging the user's health.^[58] These types of 3D printers not only need a fast and highly efficient PIS to initiate the polymerization without needing the deoxygenation step, but also the viscosity of the ink must be low enough so it can run through the vat. The inks for DLP 3D printing generally require a viscosity lower than 20 Pa.s at a shear rate of 10 to 100 s⁻¹ to be easily processed.^[59,60] Figure S9 (Supporting Information) shows the viscosity of different pre-polymeric solutions containing various amounts of PEDOT:PSS, from 0 to 2 wt.%. It can be appreciated that as the concentration of PEDOT:PSS increases in the ink, the viscosity also increases, but all of them meet the requirement to be processed by DLP. **Figure 4A** shows a schematic represen-

tation of the employed 3D printer where the ink is deposited in a vat, and through a layer-by-layer light irradiation in the Z axis, the pre-polymeric solution is photopolymerized on the platform, thus obtaining a hydrogel. A layer height of 0.15 mm and a layer exposure time of 20 s were applied as the optimal printing conditions. A honeycomb-based hydrogel was printed, with an area of 6 × 4 mm and 1 mm thickness. **Figure 4B** shows the SEM images of the shape-defined printed scaffolds with a hole size of 500 µm. The high printing resolution shows the great ability of the new proposed PIS to be employed for light-based 3D printing. Moreover, the incorporation of PEDOT:PSS CP in the final material is highly desirable for different applications such as tissue engineering, biosensors or bioelectronic devices.

3. Conclusion

In conclusion, a new photoinitiator system based on PEDOT:PSS/Rf/TEA has been developed for fast visible-light photopolymerization of water soluble acrylic monomers in the presence of PEDOT:PSS. Results indicate that PEDOT:PSS participates in the photoinitiation process, catalyzing the electron transfer between the triplet excited state of the dye (³Rf*) and the amine (TEA), increasing the photopolymerization reaction kinetics. This new PIS allows us to avoid problems commonly present in this Type II photoinitiator systems, such as slow

polymerizations and the presence of oxygen. As a result, conducting PHEA/PEDOT:PSS hydrogels have been synthesized in less than 4 min. As the PEDOT:PSS concentration increases, the electrical conductivity of hydrogels enhances up to 0.1 S cm^{-1} and they become stiffer, with Young's Modulus from 0.24 to 1.52 MPa. The new PIS was also tested for 3D printing purposes in a commercially available DLP 3D printer, obtaining a high-resolution honeycomb like structure with $500 \mu\text{m}$ hole size. In addition, the use of visible light in the photopolymerization process allows low energy consumption, room temperature treatment, non-polluting and low costs comparing with classical UV photopolymerization, which could damage user's health. In addition, the use of natural molecules (such as riboflavin) in the photoinitiation system can create more sustainable, eco-friendly and easy scalable approaches, as well as water-based inks for biomedical applications, while the majority of Type I photoinitiators are insoluble.^[61] Due to the use of visible light in this system, it is possible to use it in nanomedicine; using biocompatible monomers, it can be explored the possibility to directly photopolymerize inks and synthesize hydrogels inside the interested tissue (for tissue engineering applications, for example) without damaging the cell media. As the visible light penetration/curing depth can be up to 2 cm, direct injection of the ink into the human tissue and subsequent photopolymerization from outside can be developed as a future strategy, where the conductivity of PEDOT:PSS can accelerate cell proliferation or diagnosis of diseases can be obtained by electrocardiography (ECG) recordings. Finally, it is worth noting that these hydrogels can be very versatile as different polymer matrixes can be used to obtain thermal, light or even pH responsive materials, apart from the electrical conductivity that they may possess, and integrate them in some bioelectronic devices such as organic electrochemical transistors (OECTs).

Supporting Information

Supporting Information is available from the Wiley Online Library or from the author.

Acknowledgements

Financial support of the Spanish Agencia Estatal de Investigación of the MINECO through project PID2020-119026GB-I00 is acknowledged.

Conflict of Interest

The authors declare no conflict of interest.

Data Availability Statement

Research data are not shared.

Keywords

3D printing, conducting polymers, hydrogels, PEDOT:PSS, Type II photoinitiator system, visible-light photopolymerization

Received: April 24, 2023

Revised: June 1, 2023

Published online: July 2, 2023

- [1] H. Yuk, B. Lu, X. Zhao, *Chem. Soc. Rev.* **2019**, *48*, 1642.
- [2] F. Fu, J. Wang, H. Zeng, J. Yu, *ACS Mater. Lett.* **2020**, *2*, 1287.
- [3] A. M.-D. Wan, S. Inal, T. Williams, K. Wang, P. Leleux, L. Estevez, E. P. Giannelis, C. Fischbach, G. G. Malliaras, D. Gourdon, *J. Mater. Chem. B* **2015**, *3*, 5040.
- [4] X. Su, X. Wu, S. Chen, A. M. Nedumaran, M. Stephen, K. Hou, B. Czarny, W. L. Leong, *Adv. Mater.* **2022**, *34*, 2200682.
- [5] S. Han, N. U. H. Alvi, L. Granl f, H. Granberg, M. Berggren, S. Fabiano, X. Crispin, *Adv. Sci.* **2019**, *6*, 1802128.
- [6] D. Mawad, A. Artzy-Schnirman, J. Tonkin, J. Ramos, S. Inal, M. M. Mahat, N. Darwish, L. Zwi-Dantsis, G. G. Malliaras, J. J. Gooding, *Chem. Mater.* **2016**, *28*, 6080.
- [7] D. M. Nguyen, Y. Wu, A. Nolin, C.-Y. Lo, T. Guo, C. Dhong, D. C. Martin, L. V. Kayser, *Adv. Eng. Mater.* **2022**, *24*, 2200280.
- [8] Y. J. Jo, K. Y. Kwon, Z. U. Khan, X. Crispin, T.-I. Kim, *ACS Appl. Mater. Interfaces* **2018**, *10*, 39083.
- [9] C. Mart n, S. Merino, J. M. Gonz lez-Dom nguez, R. Rauti, L. Ballerini, M. Prato, E. V zquez, *Sci. Rep.* **2017**, *7*, 10942.
- [10] Y. Wei, Q. Zeng, M. Wang, J. Huang, X. Guo, L. Wang, *Biosens. Bioelectron.* **2019**, *131*, 156.
- [11] S. Naficy, F. Oveissi, B. Patrick, A. Schindeler, F. Dehghani, *Adv. Mater. Technol.* **2018**, *3*, 1800137.
- [12] M. Lee, R. Rizzo, F. Surman, M. Zenobi-Wong, *Chem. Rev.* **2020**, *120*, 10950.
- [13] N. Alegret, A. Dominguez-Alfaro, D. Mecerreyes, *Biomacromolecules* **2019**, *20*, 73.
- [14] M. J. Donahue, A. Sanchez-Sanchez, S. Inal, J. Qu, R. M. Owens, D. Mecerreyes, G. G. Malliaras, D. C. Martin, *Mater. Sci. Eng., R* **2020**, *140*, 100546.
- [15] A. Martinelli, A. Nitti, G. Giannotta, R. Po, D. Pasini, *Mater. Today Chem.* **2022**, *26*, 101135.
- [16] M. Criado-Gonzalez, A. Dominguez-Alfaro, N. Lopez-Larrea, N. Alegret, D. Mecerreyes, *ACS Appl. Polym. Mater.* **2021**, *3*, 2865.
- [17] H. Yuk, B. Lu, S. Lin, K. Qu, J. Xu, J. Luo, X. Zhao, *Nat. Commun.* **2020**, *11*, 1604.
- [18] B. Indranil, G. Nowicki, B. Ruttens, D. Desta, J. Prooth, M. Jose, S. Nagels, H. G. Boyen, J. D'Haen, M. Buntinx, W. Deferme, *Polymers* **2020**, *12*, 2915.
- [19] A. Dominguez-Alfaro, E. Gabirondo, N. Alegret, C. M. De Le n-Almaz n, R. Hernandez, A. Vallejo-Illarramendi, M. Prato, D. Mecerreyes, *Macromol. Rapid Commun.* **2021**, *42*, 2100100.
- [20] N. Casado, S. Zendeji, L. C. Tom , S. Velasco-Bosom, A. Aguzin, M. Picchio, M. Criado-Gonzalez, G. G. Malliaras, M. Forsyth, D. Mecerreyes, *J. Mater. Chem. C* **2022**, *10*, 15186.
- [21] M. L. Picchio, A. Gallastegui, N. Casado, N. Lopez-Larrea, B. Marchiori, I. del Agua, M. Criado-Gonzalez, D. Mantione, R. J. Minari, *Adv. Mater. Technol.* **2022**, *7*, 2101680.
- [22] D. N. Heo, S.-J. Lee, R. Timsina, X. Qiu, N. J. Castro, L. G. Zhang, *Mater. Sci. Eng., C* **2019**, *99*, 582.
- [23] R. L. Keate, J. Tropp, C. P. Collins, H. O. T. Ware, A. J. Petty, G. A. Ameer, C. Sun, J. Rivnay, *Macromol. Biosci.* **2022**, *22*, 2200103.
- [24] O. Dadras-Toussi, M. Khorrami, A. S. C. Louis Sam Titus, S. Majd, C. Mohan, M. Reza Abidian, *Adv. Mater.* **2022**, *34*, 2200512.
- [25] A. Dominguez-Alfaro, M. Criado-Gonzalez, E. Gabirondo, H. Lasa-Fern ndez, J. L. Olmedo-Mart nez, N. Casado, N. Alegret, A. J. M ller, H. Sardon, A. Vallejo-Illarramendi, D. Mecerreyes, *Polym. Chem.* **2022**, *13*, 109.
- [26] N. Lopez-Larrea, M. Criado-Gonzalez, A. Dominguez-Alfaro, N. Alegret, I. del Agua, B. Marchiori, D. Mecerreyes, *ACS Appl. Polym. Mater.* **2022**, *4*, 6749.
- [27] N. Nestler, C. Wesemann, B. C. Spies, F. Beuer, A. Bumann, *J. Prosthet. Dent.* **2021**, *125*, 103.
- [28] F. Dumur, *Eur. Polym. J.* **2023**, *187*, 111883.

- [29] B. Bao, J. You, D. Li, H. Zhan, L. Zhang, M. Li, T. Wang, *J. Photochem. Photobiol. A Chem.* **2022**, 429, 113938.
- [30] J. Lalevée, M.-A. Tehfe, F. Dumur, D. Gigmes, N. Blanchard, F. Morlet-Savary, J. P. Fouassier, *ACS Macro Lett.* **2012**, 1, 286.
- [31] X. Wu, S. Gong, Z. Chen, J. Hou, Q. Liao, Y. Xiong, Z. Li, H. Tang, *Dyes Pigm.* **2022**, 205, 110556.
- [32] W. Tomal, M. Pilch, A. Chachaj-Brekiesz, M. Galek, F. Morlet-Savary, B. Graff, C. Dietlin, J. Lalevée, J. Ortyl, *Polym. Chem.* **2020**, 11, 4604.
- [33] P. Sautrot-Ba, S. Jockusch, J. P. Malval, V. Brezová, M. Rivard, S. Abbad-Andaloussi, A. Blacha-Grzechnik, D. L. Versace, *Macromolecules* **2020**, 53, 1129.
- [34] F. Dumur, *Eur. Polym. J.* **2020**, 126, 109564.
- [35] J. P. Fouassier, X. Allonas, D. Burget, *Prog. Org. Coat.* **2003**, 47, 16.
- [36] J. Kabatc, *Photopolymerisation Initiating Systems* (Eds.: J. Lalevée, J.P. Fouassier) Royal Society of Chemistry, London **2018**.
- [37] J. Shao, Y. Huang, Q. Fan, *Polym. Chem.* **2014**, 5, 4195.
- [38] K. Sun, P. Xiao, F. Dumur, J. Lalevée, *J. Polym. Sci.* **2021**, 59, 1338.
- [39] A. Gallastegui, A. Dominguez-Alfaro, L. Lezama, N. Alegret, M. Prato, M. L. Gómez, D. Mecerreyes, *ACS Macro Lett.* **2022**, 11, 303.
- [40] I. Zaborniak, P. Chmielarz, *Eur. Polym. J.* **2021**, 142, 110152.
- [41] M. V. Encinas, A. M. Rufs, S. Bertolotti, C. M. Previtali, *Macromolecules* **2001**, 34, 2845.
- [42] Y.-Y. Liu, J. Lü, Y.-H. Shao, *Macromol. Biosci.* **2006**, 6, 452.
- [43] D. Mantione, I. del Agua, W. Schaafsma, J. Diez-Garcia, B. Castro, H. Sardon, D. Mecerreyes, *Macromol. Biosci.* **2016**, 16, 1227.
- [44] A. V. Marquez, N. McEvoy, A. Pakdel, *Molecules* **2020**, 25, 5288.
- [45] F. Dumur, *Eur. Polym. J.* **2023**, 186, 111874.
- [46] M. Modarresi, A. Mehandzhiyski, M. Fahlman, K. Tybrandt, I. Zozoulenko, *Macromolecules* **2020**, 53, 6267.
- [47] L. Bießmann, L. P. Kreuzer, T. Widmann, N. Hohn, J.-F. Moulin, P. Müller-Buschbaum, *ACS Appl. Mater. Interfaces* **2018**, 10, 9865.
- [48] C. Duc, A. Vlandas, G. G. Malliaras, V. Senez, *Soft Matter* **2016**, 12, 5146.
- [49] H. Park, X. Guo, J. S. Temenoff, Y. Tabata, A. I. Caplan, F. K. Kasper, A. G. Mikos, *Biomacromolecules* **2009**, 10, 541.
- [50] M. Karbarz, W. Hyk, Z. Stojek, *Electrochem. Commun.* **2009**, 11, 1217.
- [51] Q. Lv, M. Wu, Y. Shen, *Colloids Surf., A: Physicochem. Eng. Asp.* **2019**, 583, 123972.
- [52] A. R. Spencer, A. Primbetova, A. N. Koppes, R. A. Koppes, H. Fenniri, N. Annabi, *ACS Biomater. Sci. Eng.* **2018**, 4, 1558.
- [53] V. R. Feig, H. Tran, M. Lee, Z. Bao, *Nat. Commun.* **2018**, 9, 2740.
- [54] F. Sun, X. Huang, X. Wang, H. Liu, Y. Wu, F. Du, Y. Zhang, *Colloids Surf., A: Physicochem. Eng. Asp.* **2021**, 625, 126897.
- [55] L. E. Beckett, J. T. Lewis, T. K. Tonge, L. T. J. Korley, *ACS Biomater. Sci. Eng.* **2020**, 6, 5453.
- [56] C. Dietlin, T. T. Trinh, S. Schweizer, B. Graff, F. Morlet-Savary, P.-A. Noiro, J. Lalevée, *Molecules* **2020**, 25, 1671.
- [57] A. Oesterreicher, M. Roth, D. Hennen, F. H. Mostegel, M. Edler, S. Kappaun, T. Griesser, *Eur. Polym. J.* **2017**, 88, 393.
- [58] D. Ahn, L. M. Stevens, K. Zhou, Z. A. Page, *ACS Cent. Sci.* **2020**, 6, 1555.
- [59] Z. Chen, J. Li, C. Liu, Y. Liu, J. Zhu, C. Lao, *Ceram. Int.* **2019**, 45, 11549.
- [60] A. Schwab, R. Levato, M. D'este, S. Piluso, D. Eglin, J. Malda, *Chem. Rev.* **2020**, 120, 11028.
- [61] W. Tomal, J. Ortyl, *Polymers* **2020**, 12, 1073.